Journal of Ceramic Processing Research. Vol. 24, No. 2, pp. 406~414 (2023)
(Received 26 September 2022, Received in revised form 8 November 2022, Accepted 17 November 2022)
https://doi.org/10.36410/jcpr.2023.24.2.406

J O U R N A L O F
Ceramic Processing Research

Characterization of mechanical and tribological behavior of r-GO and hBN reinforced AZ91 hybrid metal matrix composites: NSGA approach

T. Siva[a,*] and K. Anandavelu[b]
[a]*Research Scholar, Department of Mechanical Engineering, Anna University, Tamilnadu, India*
[b]*Professor, Department of Mechanical Engineering, MRK Institute of Technology, Tamilnadu, India*

The research article reports the mechanical and tribological behavior of magnesium (AZ91) reinforced with reduced Graphene Oxide (r-GO) and hexagonal Boron Nitride (hBN). The composites are fabricated using powder metallurgy technique. Reinforcement (r-GO and hBN) powder particles were characterized using Scanning Electron Microscope (SEM) and Transmission electron microscopy (TEM). Further, the fabricated samples were characterized using Scanning Electron Microscope (SEM). The elemental composition of the composites was confirmed using Energy Dispersive Analysis (EDAX). Furthermore, the phase angles along with the crystallinity of the samples were evaluated by X-Ray Diffraction technique (XRD). By the influence of r-GO and hBN, the mechanical and tribological properties are assessed. The process parameters are used for this study are applied load, sliding velocity and applied load (5 N, 10 N, 15 N and 20 N), sliding velocity (0.5 m/s, 1 m/s, 1.5 m/s and 2 m/s) and Wt. of r-GO (0.20-0.50) with hBN kept 1% constant for all the samples. The results revealed that r-GO and hBN has mainly contributed to enhance the properties. Furthermore, the process parameters are optimized using Response Surface Methodology (RSM) integrated with Non-Domination based Genetic Algorithm (NSGA). RSM integrated NSGA optimization results provide effective tribological process parameters such as applied load (6.2 N), sliding velocity (1.2 m/s) and Wt. of hBN: r-Go (1: 0.49) would reduce the responses such as CoF and SWR simultaneously.

Keywords: AZ91, hBN: r-GO composites, NSGA, Wear analysis.

Introduction

The phase of Matrix is considered to be an important in the formation of structure of composite. A matrix function provides shape and rigidity of the structure. The reinforcement particles in composite materials improve the mechanical properties in final net product. The various mechanical and tribological properties such as tensile strength, stiffness, hardness, elongation, wear resistance, coefficient of friction etc., can be improved. The reinforcement particles benefits to improve the load carrying capacity, stiffness, excellent strength and electrical conductivity and [1]. Magnesium is one of the lightest materials in the earth, because of its low density and better strength. It is very light in nature, when compare to aluminum and steel. So it is a very good alternative candidate for aerospace and automotive applications in specific of sports goods, electronic and household industries [2, 3]. Magnesium possesses potential of high damping and excellent castability. However, the pure magnesium is considerably lesser strength particularly at working temperatures greater than 100 °C. Thus magnesium based MMCs are introduced to bring out the superior properties of magnesium's. The MMC based magnesium alloys are vastly used in various industrial divisions across the globe [4]. The corrosion behavior of the two magnesium alloys such as AZ31 and AZ91 was compared with each other. Accordingly to the investigation, it has been found that AZ91 has a good corrosion resistance compare to AZ31 [5]. Corrosion behavior of the materials showed similar changes in the graph, it was observed that AZ91 provides better protection with a slight difference compared to AZ31.The unique nature of magnesium is suitable for biomedical applications because of its biocompatibility, biodegradability, and bio-restorability. Henceforth it is used in cardiovascular and orthopedic implant applications [3]. Considering to the properties of magnesium, it has good hardness but it exhibit poor wear resistance limiting their suitability for structural and transmission components. During implants, presence of body fluid, it creates high wear rate and resulted to produce huge wear debris. It led to create an improper functioning of implant [6, 7]. The tribological properties are mainly dependent on some specific criteria such as material, reinforcement, counter material and loading conditions. Selection of reinforcement is a very crucial role in-order to improve the mechanical and tribological properties. Therefore, more efforts are made by various researchers in-order to develop the magnesium matrix hybrid composites. Particle reinforced metal matrix composites shows

*Corresponding author:
Tel : +91 9962257709
E-mail: anandavelukk@gmail.com

enriched mechanical and tribological properties when compared to parent material [8]. This was happening, because of the presence of hard refinforced particles, which resist the removal of material during experimentation. Micro/Nano sized particles are used as reinforcement generally which improves the hardness and wear resistance. Analysis of variance results revealed that tribological process parameter such as load and incorporation of nano particles have a significant dominancy on COF and WR respectively [9]. Researchers are developed the magnesium composites through various techniques such as Liquid Metallurgy (L/M), Powder Metallurgy (P/M) and infiltration. Over to that powder metallurgy is better one for ease to fabricate the composites and also material wastage is less and also to get a net clear shape [10-12]. Following to that nano sized reinforcement provides better mechanical and tribological properties when compared to micron sized particles. In past few decades, carbon based nano particles are choose as ideal reinforcement in-order to improve the mechanical and tribological properties. In general, carbon nano tubes, graphene, reduced graphene oxide which are allotropes of carbon are mainly used as reinforcement. r-GO has a sheet like structure and it has excellent strength, elastic modulus when compare to other carbon based reinforcement [13]. The experiments were conducted based on design of experiments and further analyzed using genetic algorithm [14]. Several researches show that one-factor at a time method influences the other factors. In this method, the interaction between the each factor becomes conflict. To overcome this problem, statistical methods and multifactor studies have been introduced. Among many optimization techniques, response surface methodology (RSM) is one of the effective method and adopted by several research works [15].

Now, the researchers are focused on hybrid composites fabrication and following to that analyze the performance. Hence, the current study is focused on magnesium (AZ91) hybrid metal matrix composites reinforced with r-GO and hBN. The composites were fabricated using P/M technique. The hardness and wear behavior of the composites were assessed using Vickers Micro hardness and pin-on disc apparatus. Furthermore, the tribological process parameters were optimized using multi objective optimization techniques like RSM and NSGA.

Materials and Methods

The precursor such as magnesium, r-GO and hBN was purchased from M/S. Sigma Aldrich, Germany. Figs. 1(a-c) show the as received SEM micrograph of magnesium, r-GO and hBN and it clearly evident that magnesium and hBN are irregular in structure and r-GO are sheet like structure. For this study five different composite samples were fabricated namely a) Pure AZ91, b) AZ91+1 hBN +0.2r-GO, c) AZ91+1 hBN +0.3 r-GO, d) AZ91+1 hBN +0.4 r-GO and e) AZ91+1 hBN +0.5 r-GO through powder metallurgy technique. However, in-order to evaluate the r-GO size, TEM with line mapping analysis is pertained and it confirmed that the size of the r-GO is in nanometer range and the corresponding fig. is shown below. From the TEM Fig.

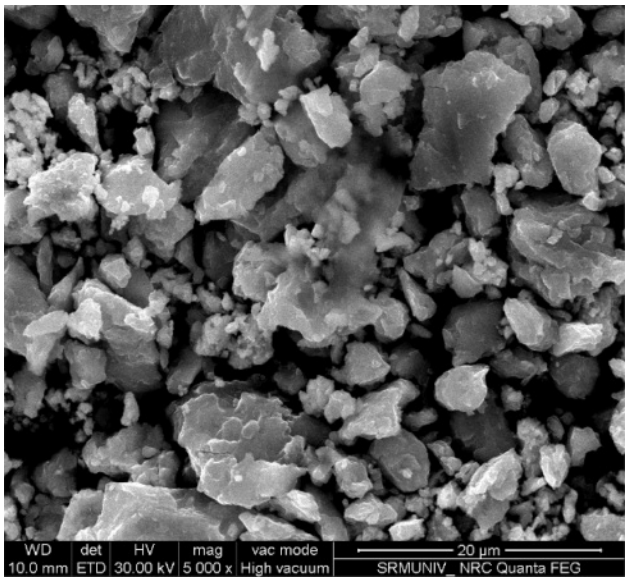

Fig. 1. SEM micrograph of as-received powder of AZ91.

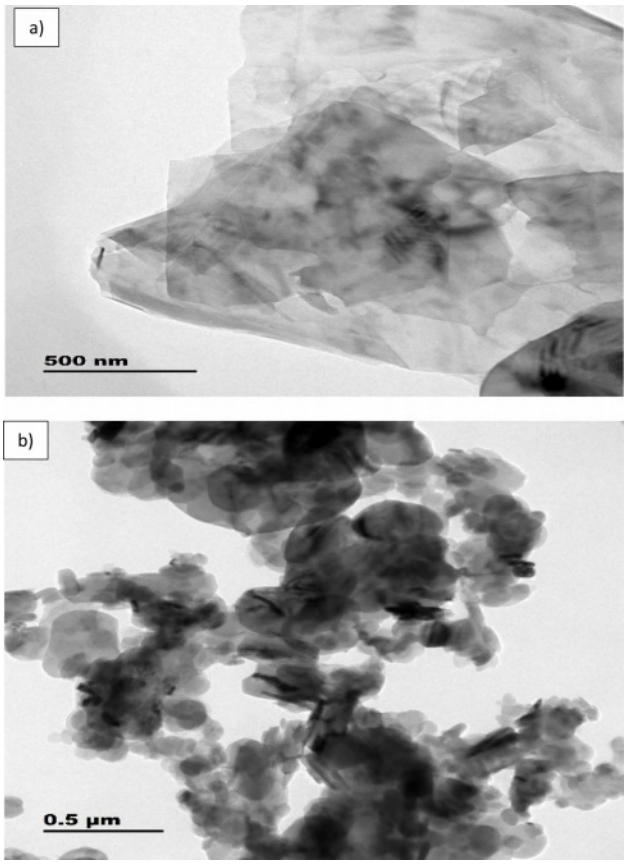

Fig. 2. TEM micrographs a) TEM of r-GO a) and b) TEM of hBN.

2(a), illustrates that, the pertained r-GO is in nano range and further two different colors namely blue is illustrate the carbon (C) and brown is displayed as oxygen (O). Also SEM Fig. 2(b), illustrates that, the pertained hBN is in micro range and further three different colors observed in EDS mapping namely blue is illustrate the boron (B), red is nitrogen (N) and green is displayed as oxygen (O).

Initially, the pre-determined powders were mixed by ball milling for 1h to attain homogenous mixture. The green compacts of the powders were fabricated using compression testing machine. Afterwards, the green compacts were sintered for 400°C using muffle furnace. The sintered samples were polished using various grit size papers such as 400, 800 and 1000 microns. Afterwards, the sintered samples underwent SEM analysis for visualize the secondary particle dispersion in the matrix. From the Fig. 3(a and b) the secondary particles such as hBN and r-GO were homogenously dispersed in the matrix. But it not confirmed the exact presence and quantity. So further, the sintered samples elemental presence was confirmed using EDAX analysis and displayed in Fig. 4(a). Here all the elements were present such as Mg, Al, Zn, B, N, C and O. However, the Mg intensity is high which means that the amount

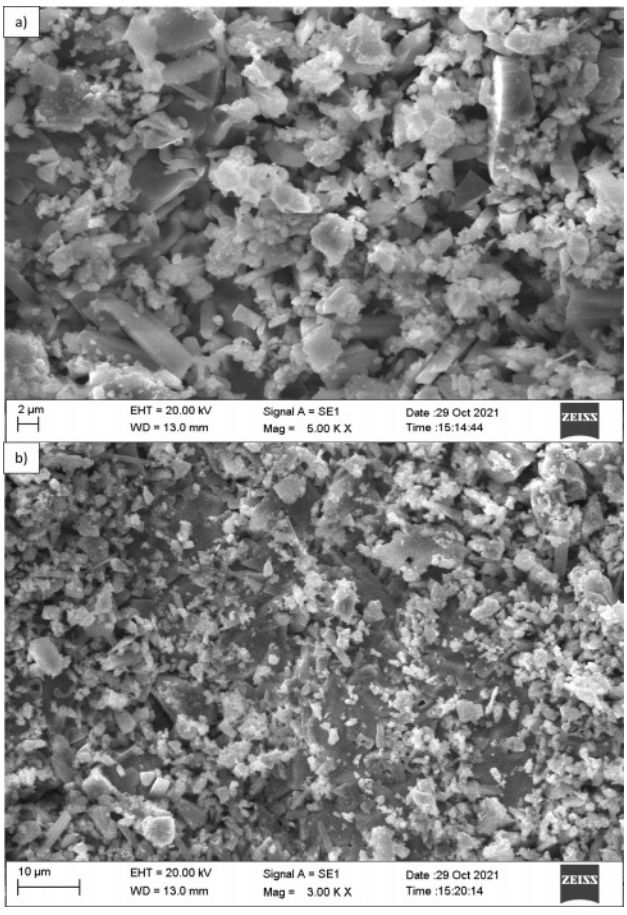

Fig. 3. SEM Image of sintered samples a) AZ91+1 hBN +0.2 r-GO and b) AZ91+1 hBN +0.5 r-GO

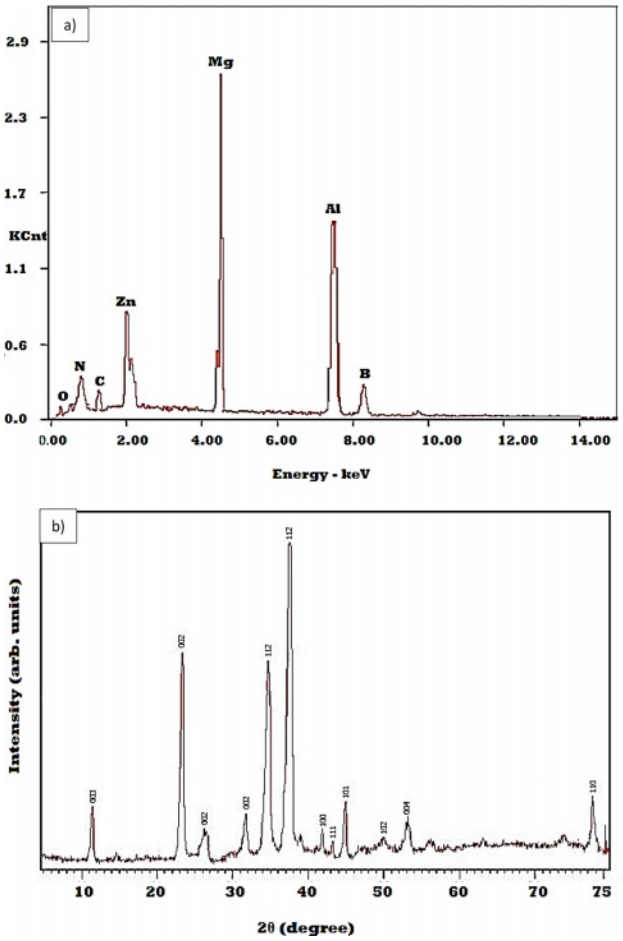

Fig. 4. a) EDAX spectrum for AZ91+1 hBN+0.5r-GO composites and b) XRD spectrum for the same

of Mg is high in the composites. After that, the intensity levels are decreased for all the other alloying elements. Fig. 4(b) shows the XRD spectrum of AZ91+1 hBN +0.5 r-GO. Here the miller indices for Mg AZ 91 is (003), (002) and (112), hBN is (002), (100), (101), (102), (004) and (110) and r-GO is (002), (111). It confirms that all the alloying elements were present and these are in crystalline nature.

The fabricated composites were undergone tribological behavior using Pin-on-disc apparatus. The process parameters are used for this study are applied load (5 N, 10 N, 15 N and 20 N), sliding velocity (0.5 m/s, 1 m/s, 1.5 m/s and 2 m/s) and Wt. of r-Go (0.20-0.50) with hBN kept 1% constant for all the samples respectively. Sliding distance is kept constant for throughout the experiment (1000 m). The output responses such as specific wear rate and coefficient of friction was calculated based upon the following equations (1) and (2). Table 1 portrays the selection of tribological process parameter ranges. The ranges of process parameters were selected based on the preliminary research work. The Table 2 shows the design of experiments (DoE) developed using central composite design of response surface methodology (RSM).

Table 1. Ranges of tribological process parameters.

	Name	Units	Low	High	–alpha	+alpha
A [Numeric]	Applied load	N	6	18	6	18
B [Numeric]	Sliding velocity	m/s	0.4	1.6	0.4	1.6
C [Numeric]	Wt. of HBN : r-Go	%	0.2	0.5	0.2	0.5

Table 2. Design of experiments.

Sl.No	A:Applied load	B:Sliding velocity	C:Wt. of hBN : r-Go	SWR × (10^{-4})	CoF
1.	N	m/s	%	mm^3/N-m	
2.	6	1.6	1:0.50	0.81	0.22
3.	12	1	1:0.50	0.88	0.23
4.	6	1	1:0.35	0.99	0.25
5.	12	1.6	1:0.35	1.12	0.26
6.	12	1	1:0.35	1.49	0.3
7.	12	1	1:0.35	1.56	0.31
8.	12	1	1:0.35	1.79	0.33
9.	6	0.4	1:0.20	1.87	0.36
10.	12	1	1:0.35	1.9	0.37
11.	12	1	1:0.35	2.12	0.39
12.	12	0.4	1:0.35	2.32	0.4
13.	18	1	1:0.35	2.49	0.42
14.	12	1	1:0.20	2.52	0.45
15.	18	1.6	1:0.50	2.68	0.49
16.	18	0.4	1:0.50	2.7	0.51

$$\text{Specific wear rate} = \text{Volume loss/Applied load} \times \text{Sliding distance} \quad (1)$$

$$\text{Coefficient of friction} = \text{Frictional force/Applied load} \quad (2)$$

Results and Discussion

Statistical Analysis

Design expert software V.11 is used for response surface methodological (RSM) study. Statistical analysis was studied using experimental values from DoE of RSM. The percentage of contribution has been analyzed using analysis of variance (ANOVA). ANOVA helps to identify the most influencing tribological process parameter. The ANOVA is used to identify the impact of individual factors. The P-value helps to indicate the individual factor based on statistically importance. Each input factors in the ANOVA has to be evaluated and the each factors p-value is found to be lower than 0.05, then the particular input factor is considered as statically significant. The most influencing tribological process parameters were accessed from the F- statistical values. The SWR F- statistical values for applied load (19.3), sliding velocity (12.77) and wt. of hBN: r-Go (23.73). From the F- statistical values (SWR), it has been observed that wt. of hBN: r-Go influences at maximum for specific wear rate. The statistical analysis values observed for CoF is applied load (10.46), sliding velocity (7.46) and wt. of hBN: r-Go (18.24). From the F- statistical values (CoF), it has been observed that wt. of hBN: r-Go influences at maximum for specific wear rate. Overa;; statistical analysis shows that addition of reinforcement particles hBN: r-Go plays a significant role compare to all other tribological process parameters. The most common interpretation of the coefficient of determination (R^2) is used to interpret how well the developed regression model fits the experimental data. The R^2 values for SWR (98%) and CoF (99%) shows the good coefficient of determination for predicted results. The predicted versus experimental Figures shows the minimum error occurrence of predicted analysis.

Hardness

Fig. 5 shows the hardness of the fabricated hybrid composites and it illustrates that the continuous improvement in the hardness while reinforcing the secondary particles. By the hardness is concern, the secondary particles were properly dispersed in the

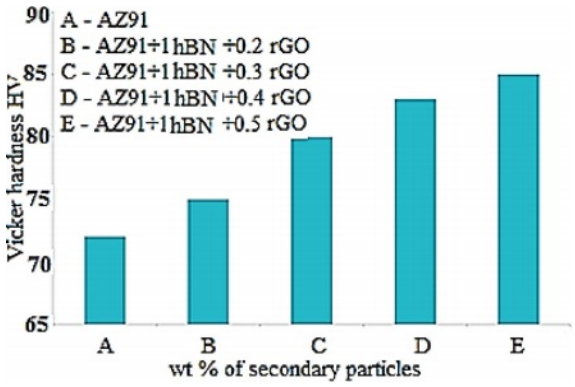

Fig. 5. Variation of hardness of AZ91 hybrid composites.

matrix medium and it endure the hardness. Over to that AZ91+1rGO+0.5 hBN possessed better hardness having in the range of 85 HV. In the other hand, the density is also measured for fabricated composites using Archimedes' principle and it clearly reveals that the relative density is greater than 90%. Henceforth the porosity is less than or equal to 10%. This is also the main factor, for the improvement of hardness [16].

Variation of specific wear rate over to applied load and sliding velocity

Fig. 6(a & b) contour plot graph shows the variation of specific wear rate with respect to applied load and sliding velocity. It was observed from the contour plot graph, the red color shows the peak SWR value about 2.7×10^{-4} mm^3/N-m and blue color shows the minimum value of SWR about 0.81×10^{-4} mm^3/N-m. According to Fig. 6(a), applied load is concern, increasing the load, will lead to increase the specific wear rate, irrespective of the composites. Fig. 6(b) portrays that minimum SWR could achieve at preference of maximum amount of reinforcement ceramics (1% rGO+0.5% hBN). The ceramic particles act a leading role in the fabricated composites and tern to reduce the specific wear rate. It was happening, because of the homogenous dispersion of hard ceramic particles. It acts as block and to evade the contact between the composites and counter disc. During sliding, initially the evade was high for composites and counter disc. It increases the specific wear rate. But, reinforcement of hard ceramic particles, gives a protective layer between the composites and counter surface. It reduces the specific wear rate, irrespective of the wt.% of the hard ceramic particles. Over to that, AZ91+1rGO+0.5 hBN possessed better wear resistance property than other composites. As for as sliding velocity as concern, increasing the sliding velocity, will leads to reduce the specific wear rate for all the fabricated composites [16-18]. It was happening, because of increasing the sliding velocity, the contact between the composites and counter disc in not in proper manner. It leads to reduce the specific wear rate.

Variation of Coefficient of friction over to applied load and sliding velocity

Fig. 7(a & b) contour plot graph shows the variation of specific wear rate with respect to applied load and sliding velocity. It was observed from the contour plot graph, the red color shows the peak CoF value about 0.51 and blue color shows the minimum value of CoF about 0.22. According to Fig. 7(a), applied load is concern, increasing the load, will lead to increase the coefficient of friction, irrespective of the composites. Fig. 7(b) portrays that minimum CoF could achieve at preference of maximum amount of reinforcement

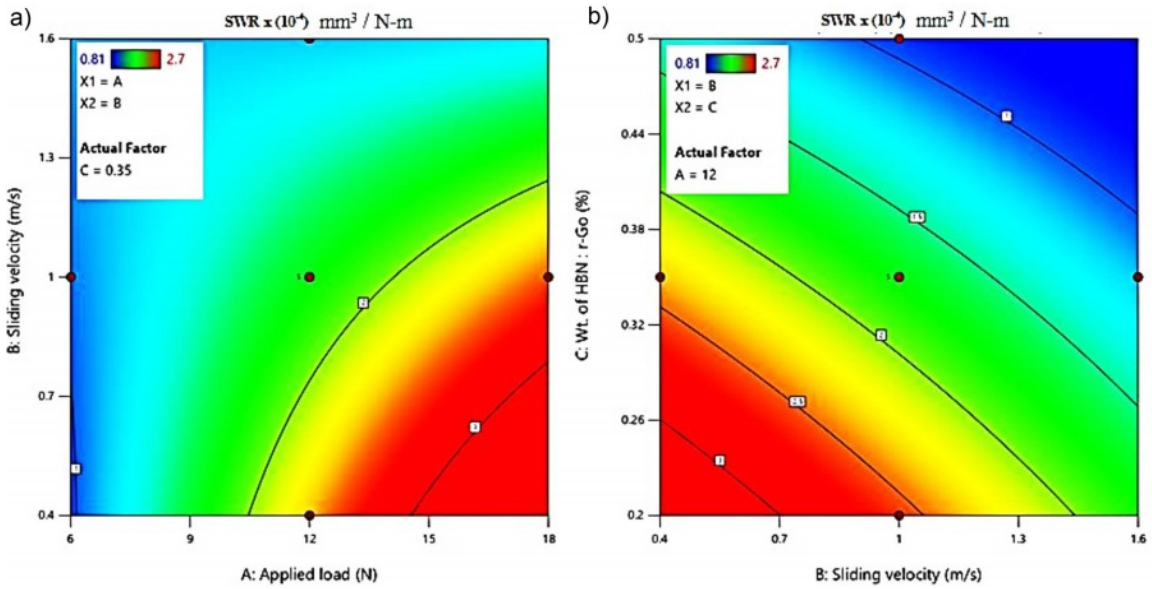

Fig. 6. Contour plot of specific wear rate a) applied load and b) sliding velocity.

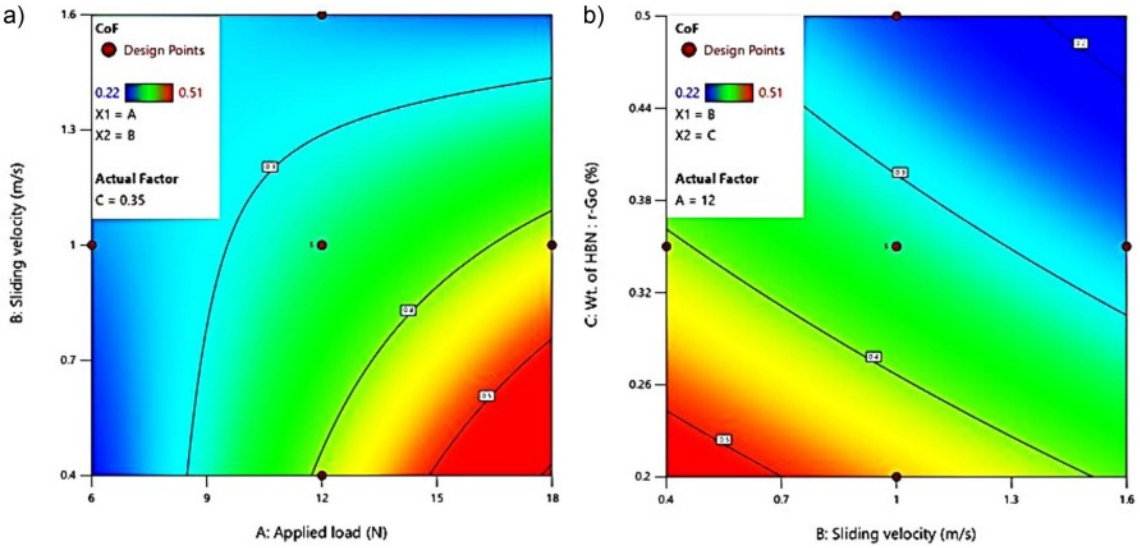

Fig. 7. Contour plot of coefficient of friction over to a) applied load and b) sliding velocity.

ceramics (1% rGO+0.5% hBN). The ceramic particles act a leading role in the fabricated composites and tern to reduce the coefficient of friction. The applied load, gives pressure between the composites and counterpart. It increases the friction between the composites and counterpart. Synergistically, the heat is also increased between the composites and counterpart. It also increases the coefficient of friction. But the hard ceramic particle act as evade and reduce the coefficient of friction. However, the generation of heat creates the oxides between the composites and counter disc. These oxides are propagated and create a layer between the composites and counter disc. It also acts as a barrier between the composites and counter disc and reduces the coefficient of friction [16-18]. Over to that, AZ91+1rGO+0.5 hBN possessed less coefficient of friction than other composites.

As for as sliding velocity as concern, increasing the sliding velocity, will leads to reduce the coefficient of friction for all the fabricated composites. It was happening, because of increasing the sliding velocity, the contact between the composites and counter disc in not in proper manner. It leads to reduce the coefficient of friction.

Worn surface analysis

The structure of graphene acts as a self-lubricating layer in process of metal matrix composites which improves the wear resistance [19]. Figs. 8(a-e) show the wear surface scanning electron micrograph of fabricated composites. It is clearly evident that adhesion wear mechanism is happening for pure AZ91 composites. However, AZ 91 composite is ductile in nature. So that severe plastic deformation is happened for those composites. It also correlates with Fig. 6. Increasing the reinforcement wills leads to reduce the specific wear rate and also some craters and pits were visualized in the surface of those composites. Fig. 8(b) shows the AZ91+1rGO+0.2 hBN composites. The carbon based ceramic particle and the hBN particles are sprinkled along the sliding direction. It clearly visualized in the Fig. 8(b). It reduces the specifc wear rate. Figs. 8(c & d) show the surface morphology of AZ91+1rGO+0.3 hBN & AZ91+1rGO+0.4 hBN composites. Some of the craters are seen in the surface and clusters are also perceived in the surfaces [20, 21]. It also reduces the friction and wear. Fig. 8(e) shows that large amount of pits and delamination wear is also observed in that surfaces. It reduces the plastic deformation following to that it reduces the specific wear rate and coefficient of friction. It also very closely associated with Figs. 6 and 7.

Multi objective optimization using NSGA

The multi-objective optimization helps to find the optimal results of more than one desired objectives [22, 23]. The optimal parameter selection is challenging task. Non-Domination based Genetic Algorithm (NSGA) is the efficient random-based evolutionary algorithms (EAs) adopted in this research work [20]. The CoF and SWR mathematical equations (3) and (4) developed from RSM statistical analysis were used to find the optimal solutions using Non-Domination based Genetic Algorithm (NSGA). The equations are used to predict the optimal solutions for the responses CoF and SWR simultaneously which is in terms of actual factors for given levels of each factor. NSGA multi objective optimization problem was done using MATLAB version. 7 with constrain functions. The GA parameters selected for multi objective optimizations are constraints - 2, objectives - 3, size of population - 20, generation attained - 451, mutation function 0.8 and crossover - 0.01

The combined possibility results of tribological wear

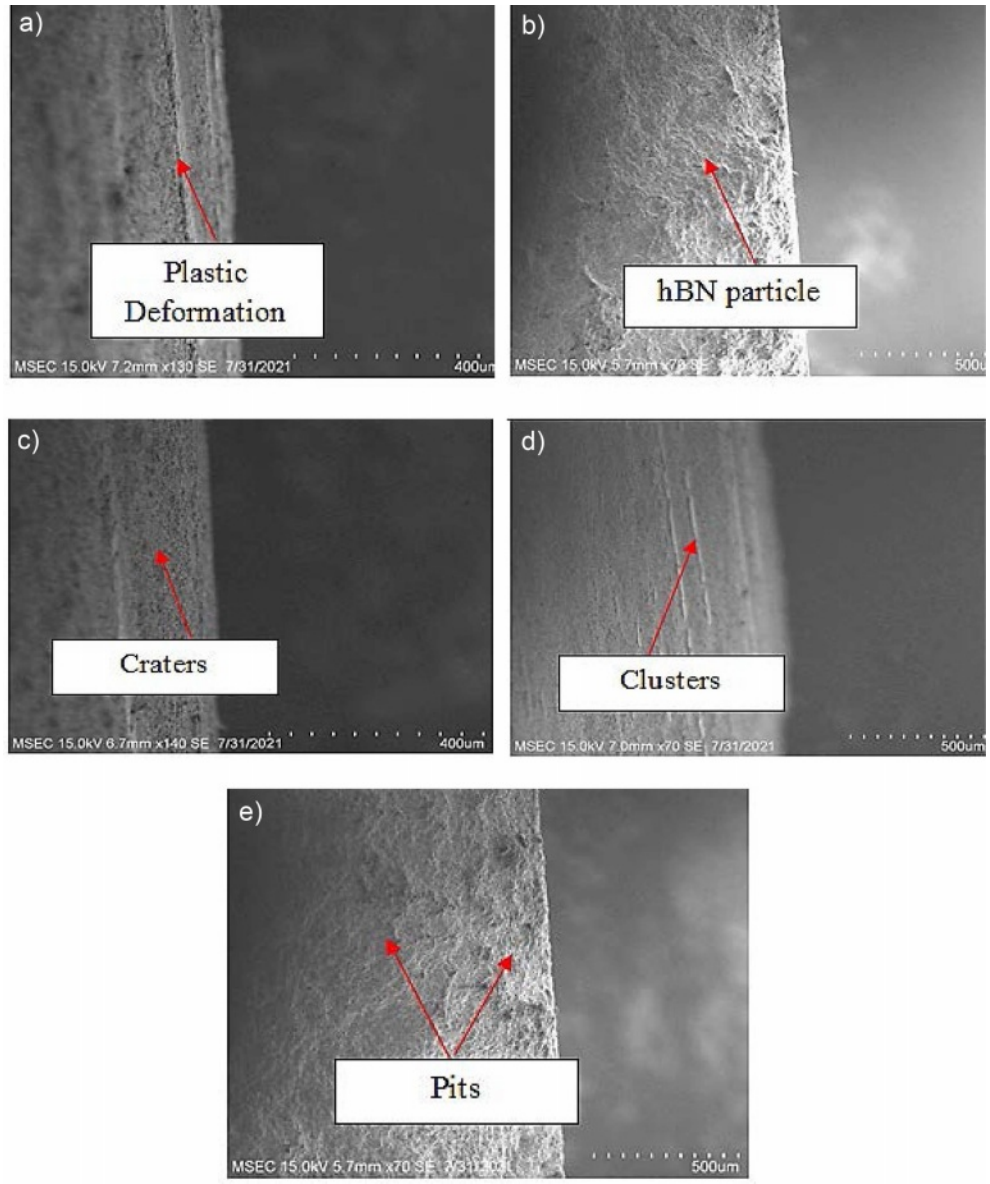

Fig. 8. Worn surface SEM micrograph a) Pure AZ91, b) AZ91+1 hBN +0.2r-GO, c) AZ91+1 hBN +0.3 r-GO, d) AZ91+1 hBN+0.4 r-GO and e) AZ91+1 hBN +0.5 r-GO.

analysis process parameters such as applied load, sliding velocity and Wt. of hBN: r-Go for the responses fun1 (CoF) and fun2 (SWR) were shown in Fig. 9. The NSGA procedure follows:

{{ Function fun = NSGA_optimization SWR & CoF;

$$\text{SWR} \times (10^{-4}) = 1.2005615485238 + 0.36070415897199 \times \text{Applied load} + 0.34834912221512 \times \text{Sliding velocity} - 6.200102102422 \times \text{Wt. of hBN : r-Go} - 0.19781508215546 \times \text{Applied load} \times \text{Sliding velocity} - 0.21300385325662 \times \text{Applied load} \times \text{Wt. of hBN : r-Go} + 2.3699614674338 \times \text{Sliding velocity} \times \text{Wt. of hBN : r-Go} + 0.0014891564268295 \times \text{Applied load}^2 + 0.0933600871274 \times \text{Sliding velocity}^2 + 1.2608850060374 \times \text{Wt. of hBN : r-Go}^2 \quad (3)$$

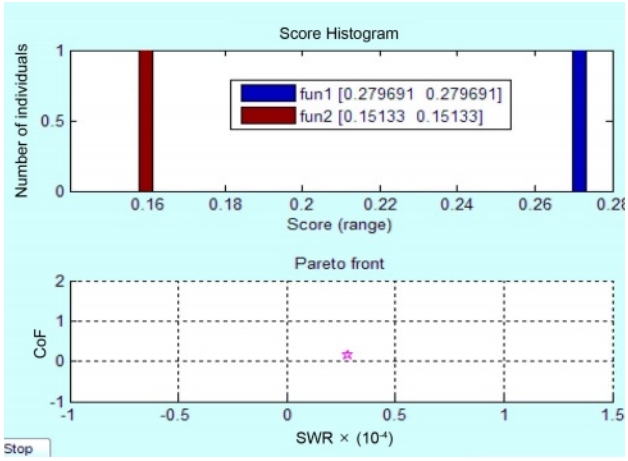

Fig. 9. Optimized results using NSGA.

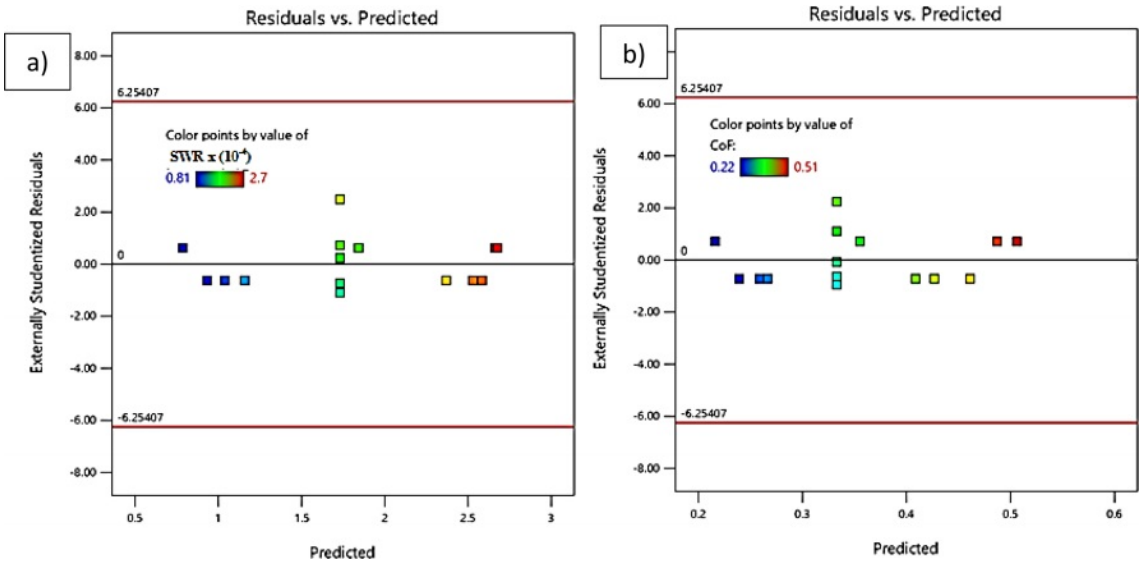

Fig. 10. Residual versus predicted plot of a) SWR and b) CoF.

CoF = + 0.32660274167199 + 0.039248230224685 × Applied load + 0.19353528896465 × Sliding velocity – 1.2655775741648 × Wt. of hBN : r-Go – 0.029787271823283 × Applied load × Sliding velocity -0.0057366763737956 × Applied load × Wt. of hBN : r-Go + 0.053744347373157 × Sliding velocity × Wt. of hBN : r-Go + 0.00027307218789213 × Applied load^2 + 0.013418329900324 × Sliding velocity^2 + 0.77278215782371 × Wt. of hBN : r-Go^2 (4)

Within the constraint limits: Applied load (6 to 18) N;

Sliding velocity (0.4 to 1.6) m/s;

Wt. of HBN: r-Go (0.2 to 0.5) %;

Objective of the function: Minimize (SWR); Minimize (CoF); }}

The Fig. 10 portrays that minimum specific wear rate about 0.15 × 10^{-4} mm^3/N-m and minimum coefficient of friction 0.27 could be achieved towards tribological wear analysis process parameters such as applied load (6.2 N), sliding velocity (1.2 m/s) and Wt. of hBN: r-Go (1 : 0.49). The Fig. 10, residual versus predicted plot clearly reveals that residual points were very closely lies with the predicted points on mean line which shows that the predicted values are highly satisfactory [24].

Conclusion

- Increasing the wt.% of the secondary particles leads to increase the hardness and the maximum of hardness was obtained as 85 HV for AZ91+1rGO +0.5 hBN composites.
- According to applied load as concern, increasing the applied load will leads to increase the specific wear rate and coefficient of friction irrespective of the composites. However, AZ91+1 hBN+0.5rGO perceived that the minimum specific wear rate over to other composites.
- According to sliding velocity as concern, increasing the sliding velocity will leads to decrease the specific wear rate and coefficient of friction irrespective of the composites. However, AZ91+1 hBN+0.5rGO perceived that the minimum coefficient of friction over to other composites.
- Many pits and delamination wear was observed for AZ91+1 hBN+0.5rGO composites. It reduces the plastic deformation and led to reduce the specific wear rate and coefficient of friction.
- RSM integrated NSGA optimization results shows effective tribological process parameters such as applied load (6.2 N), sliding velocity (1.2 m/s) and Wt. of hBN: r-Go (1: 0.49) which reduces CoF and SWR simultaneously.

References

1. K.M. Senthilkumar, A. Sivakumar, R.M. Shivaji, S.K. Tamang, and M. Giriraj, J. Ceram. Process. Res. 23[2] (2022) 233-236.
2. X. Yuan, G. Li, X. Zhang, J. Pu, and P. Ren, Wear 462 (2020) 462-463.
3. V. Manakari, G. Parande, M. Doddamani, and M. Gupta, Ceram. Int. 145[7] (2019) 9302-9305.
4. R. Sivabalan, K.R. Thangadurai, and K. Lenin, J. Ceram. Process. Res. 22[6] (2021) 605-614.
5. B. Mehmet, S. Baslayici, and A.Ç.M.A.M. Ercan, J. Ceram. Process. Res. 22[1] (2021) 98-105.
6. S.J. Huang, A. Abbas, and B. Ballokova, J. Mater. Res. Technol. 8[5] (2019) 4273-4286.
7. L. Qingyang, Z. Qinqin, and A. Maozhong, Materialia 4 (2018) 282-286.

8. K. Kaviyarasan, R. Soundararajan, P. Seenuvasaperumal, A. Sathishkumar, and J.P. Kumar, Mater. Today: Proc. 18 (2019) 4802-4091.
9. A. Kanakaraj, R. Mohan, and R. Viswanathan, J. Ceram. Process. Res. 23[3] (2022) 268-277.
10. F. Mert, Trans. Non-ferr. Met. Soc. China 27[12] (2017) 2598-2606.
11. E. Ilanaganar and S. Anbuselvan, Mater. Today: Proc. 5[1] (2018) 628-635.
12. M. Bo, Z, Xing, L.M. Pradeep, and L. Yiliang, Materialia 8 (2019) 100444.
13. M.A. Gomez-Alvarez, A. Diaz, I. Mota, V. Cabrera, and L. Resendiz, Dig. J. Nanomater. Biostructures 16[1] (2021) 101-107.
14. N. Zeelanbasha, V. Senthil, and G. Mahesh, Int. J. Oper. Res. 38[2] (2020) 221-254.
15. M. Abolfazli and M.H. Paydar, J. Ceram. Process. Res. 23[2] (2022) 188-198.
16. A. Aatthisugan, R. Rose, and D.S. Jebadurai, J. Magnes. Alloys 5[1] (2017) 20-25.
17. J. Jie, L. Huan, and L. Xiaohan, Rare Met. Mater. Eng. 46[5] (2017) 1202-1206.
18. Y. Yingxia, H. Bolin, L. Zongmin, L. Siyong, and X. Songsong, Rare Met. Mater. Eng. 46[7] (2017) 1798-1802.
19. V. Kavimani, K.S. Prakash, and T. Thankachan, Surf. Interfaces 6 (2017) 143-153.
20. P. Narayanasamy and N. Selvakumar, Trans. Non-ferr. Met. Soc. China 27[2] (2017) 312-323.
21. M.E. Turan, Y. Sun, and Y. Akgul, J. Alloys Compd. 740 (2018) 1149-1158.
22. N. Ravikumar, R. Vijayan, and R. Viswanathan, J. Ceram. Process. Res. 24[1] (2023) 142-152.
23. S. Raja, K. Vignesh, M. Ravikumar, and R. Sanjeevi, J. Ceram. Process. Res. 24[1] (2023) 153-157.
24. R. Santhanakrishnan, V.S. Thangarasu, R. Arravind, and V. Ramachandira, J. Ceram. Process. Res. 24[1] (2023) 174-181.